Proc. of the 9th Intl. Conf. of Asian Society for Precision Engg. and Nanotechnology (ASPEN 2022)
15–18 November 2022, Singapore. Edited by Nai Mui Ling Sharon and A. Senthil Kumar
doi://10.3850/978-981-18-6021-8_OR-02-0216

Design and Development of a Concrete Surface Roughness Assessment Device

Muhammad Qaihri Bin Wahab[1], and Mustafa Shabbir Kurbanhusen[1,#]

1 Engineering Cluster, Singapore Institute of Technology, 10 Dover Drive, 138683, Singapore
Corresponding Author / Email: Mustafa.Shabbir@Singaporetech.edu.sg, TEL: +65 6592 2190

KEYWORDS: Mechatronics, Gantry Robot, Surface Assessment

In the construction industry, concrete surface grinding tasks result in a very dusty environment, posing health and safety risks to the workers. There are semi-automated and automated robotic solutions which aim to alleviate the strenuous polishing/grinding work through the use of supporting mechanisms, and even incorporating a vacuum system with the aim of minimizing the dust produced. However, the feedback of the grinding task is still done manually through visual and tactile means. This means that the automated solutions are still reliant on the human worker to provide the feedback. Looking to address this gap, this paper presents the design and development of a concrete surface roughness assessment device, based on a planar two degrees-of-freedom gantry robot configuration and fitted with a CMOS infra-red sensor to measure the surface depth. A hand-held prototype was developed, and the trial results indicated that the device was able to capture the man-made bulges and depressions at a mean distance of 10 cm of varying depths (up to a few centimeters) with measurement accuracy of approximately 5%.

1. Introduction

Concrete grinding is a very common process in the construction industry that utilizes an abrasive media to smoothen out uneven concrete surfaces. The pre-grinding inspection process is primarily carried out via a visual and tactile inspection by a human surveyor to indicate the regions requiring grinding. The post-grinding inspection is also similarly conducted by a human surveyor. This method is subjective because it primarily relies on the human workers' level of competence [1]. In addition, low visibility and dusty conditions may lead to inferior judgment. If semi-automated or automated systems are to be used in complement with the human worker, the feedback on the surface roughness is still reliant on the human worker and this presents a need to develop a handheld surface roughness assessment device.

Analyzing the feasibility for such measurement tasks, the measurement of an evenly distributed micro-irregularities on the surface texture is known as surface roughness. It is determined by the variations in the height of the surface abnormalities, such as concavities and convexities [2]. By using this roughness parameter, it is possible to evaluate the characteristic of the concrete surface in a uniform way. For a quantitative approach to characterize the surface roughness, roughness parameters based on the geometrical properties of the surface are required, such as height, spacing, and depth. For the sake of simplicity, this evaluation uses Average Roughness (Ra), which is the most commonly used roughness parameter. The average deviation of the profile from its mean or reference line is used to calculate the average roughness. The parameter does not, however, reveal the localization of the computed variability, but mainly the roughness characteristic of the entire profile. In order to characterize a surface's variability, root-mean-square roughness is another parameter that will be used in the surface roughness assessment.

In the following sections, this paper will detail the design and development of a concrete surface roughness assessment device, including the post-processing and visualization of the surface scanning data.

2. Design of Surface Roughness Assessment Device

The surface roughness assessment device was conceptualized to be a planar two degrees-of-freedom system, based on a gantry robot configuration, actuated with stepper motors and using a CMOS infrared laser sensor to conduct the surface assessment.

2.1 Key Design Criteria

Prior to designing the measurement device, the design criteria were compiled in consultation with industry end-users, as shown in Table 1. Selection of hardware components were performed to effectively fulfil the needs of the required specifications for the scanning device. The main criteria to consider consisted of the resolution of the measurement sensor for depths of up to 0.1mm, positioning accuracy of 0.01mm and portability to facilitate in ease of use by the human worker.

Table 1 Design criteria and product specifications

No.	Criteria	Product Specifications
1	High Resolution	Able to read to 0.1mm
2	Wide Measuring Distance	Up to 150mm in the X & Y axis
3	High Positioning Control	To obtain precise movement(0.01mm intervals)
4	Portable	Less than 5kg for the overall device
5	High Durability	Low Maintenance required(last for > 1year)
6	Dustproof/Waterproof	IP Rating 65
7	Low Power Consumption	Able to use for 2-3 hours
8	Large Storage Space	Able to store about 256GB in SD cards
9	Customizable	Simple Design with detachable parts included

2.2 Key Hardware Components

As shown in Fig. 1, the portable scanning device was based on a planar two degrees-of-freedom gantry robot configuration and consisted of the Arduino micro-controller linked to stepper motors, actuated by leadscrews for the vertical axis, and a belt-and-pulley transmission for the horizontal axis. For the measurement sensor, a Complementary Metal-Oxide Semiconductor (CMOS) infrared sensor (Model: Omron ZX1-LD50A61) was utilized to measure the height of the scanning surface. The Arduino microcontroller also dualled up to serve as a data logger and processor for the sensor readings. While the data was being extracted, the average profile roughness was also simultaneously calculated in Arduino in a bid to optimize the computational effectiveness and display of the surface readings.

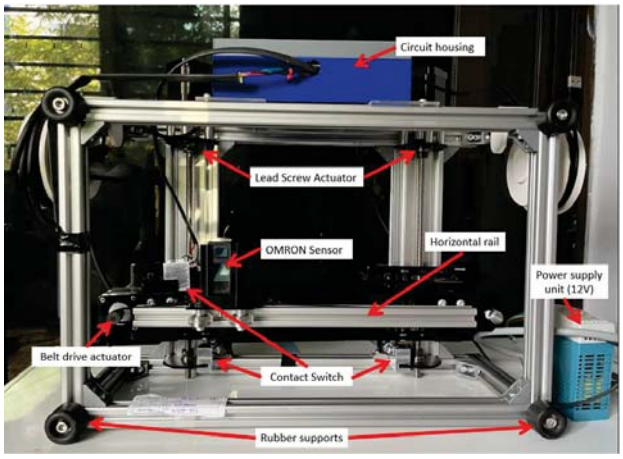

Fig. 1 Planar two degrees-of-freedom Inspection Device

2.3 Surface Roughness Sensor and Scanning Path

When choosing the appropriate surface roughness measurement sensor, the detecting range, the resolution, and the spot size were the crucial factors in consideration. These considerations were met by OMRON's Complementary Metal-Oxide Semiconductor (CMOS) infrared sensor (Model: Omron ZX1-LD50A61) with a resolution of 2μm.

The datapoints for each variation in the surface profile were recorded during the scan in order to measure the surface roughness. In order to maximize the measuring range of 40–60mm, the suitable distance between the sensor and the surface was selected to be 50mm (see Fig. 2). In addition, the sensor was developed with a 'Zero reset' function to set the reference distance to zero. Any captured bulge on the surface would show a positive height displacement after the reference surface was adjusted to zero, whereas any surface depressions would reflect as a negative height displacement.

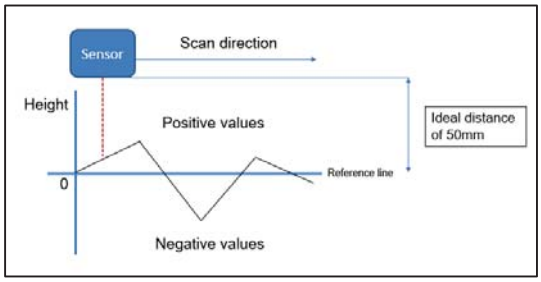

Fig. 2 Scanning schematic

The surface of interest would be scanned using several lines of varied heights in a raster scanning motion sequence (see Fig. 3). For post-processing of the roughness characteristics from the surface scanned, datasets of the surface profiles collected would be extracted and verified.

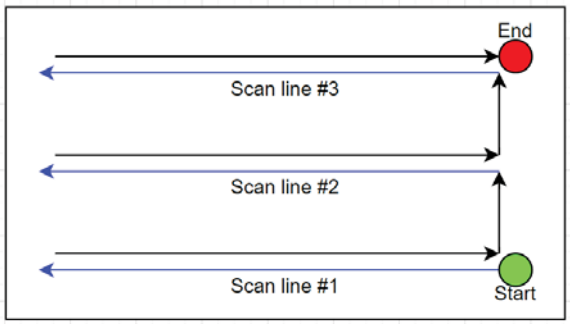

Fig. 3 Scanning pattern trajectory/path

2.4 Motion Control Implementation

In order to carry out the surface scanning, the measurement sensor would require two motion, one in the vertical axis (i.e., Y-axis) and another in the horizontal axis (i.e., X-axis), both covering a planar surface. The sensor holder holding the laser displacement sensor would move in a horizontal, linear direction and powered by a stepper motor via a belt-driven actuator. For the horizontal motion, a SilentStepStick TMC2130 motor driver and a Sparkfun hybrid stepper motor were employed. As for the vertical motion, lead screw actuators were used due to its ability to elevate higher load and the self-locking mechanism to prevent any freefall of the laser in the event of any fault. Table 2 presents the overview of the actuator and transmission selection for the two

motion.

A homing sequence was also created in order to accurately locate the sensor, prior to each scanning task. Contact switches were incorporated into the design at certain locations (see Fig. 1) to provide input on the sensor's positioning. This sequence not only determines the position of the sensor but also serves as a calibration phase for the vertical alignment of the horizontal platform. The platform must be horizontal to enable accurate representation of the surface since vertical motion is controlled by two lead screw actuators that are driven by two independent stepper motors. Also, a simple levelling test was performed, and the result showed that no tilting was observed during the vertical elevation and lowering.

Table 2 Actuator selection for X (horizontal) and Y (vertical) axes

Movement	Actuator Type	Advantages	Disadvantages
X-Axis	Timing Belt	- High Efficiency (90%) - High Speed(up to 3-5m/s) - Suited for continuous motion	- Low accuracy and positional repeatability - More input torque required
Y-Axis	Lead Screw	- High accuracy and positional repeatability - Self-Locking Mechanism -Suitable for High Load Applications	- Limited speed - Not suited for continuous motion

3. Experimental Trials and Results

For the purposes of experimentation and testing, the handheld measurement device was set on a level surface. Then, different samples of varying bulges and depressions were laid out on a flat scanning surface. The maximum scanning area of the setup measured approximately 20 cm (horizontally) by 10 cm (vertical). Start and emergency stop buttons were implemented as functional buttons for the user. Four rubber supports on the device were in contact with the area of interest and formed the scanning reference plane for the scan (see Fig. 4).

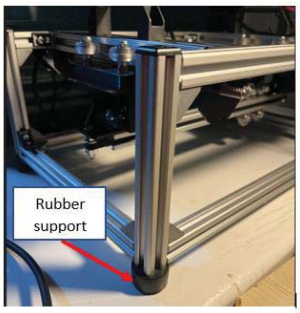

Fig. 4 Rubber support in contact with the scanning surface and serving as a datum point

3.1 Samples with various protruding heights (bulges)

The first experiment was conducted on five samples with different protruding heights (i.e., bulges) to establish the capability of the device in identifying the height of bulges (see Fig. 5). In order to remove any undesirable errors from uneven surfaces or inconsistent measurement, scanning was done by moving the sensor across all five simulated defects in both ascending and descending order. Multiple scans were also performed on the same profile for repeatability.

The surface profile data extracted from the scan were then plotted in 2D using Excel. Each of the defects were labelled from A to E with ascending thickness (see Fig. 6).

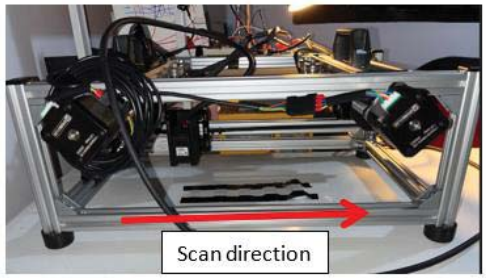

Fig. 5 Device setup on a flat table

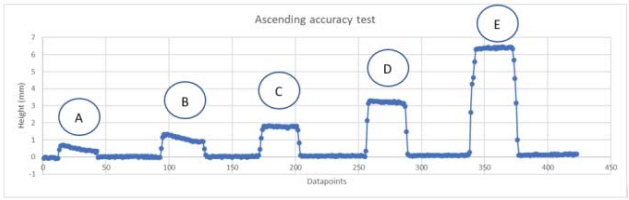

Fig. 6 Output profile plotted in Excel

These samples were first measured using a vernier caliper with a range of 0.4mm to 6mm in order to validate its accuracy. The actual measurement of the sample measured by vernier caliper were 0.49mm, 1.07mm, 1.75mm, 3.1mm, and 6.1mm, respectively, which represented the exact height of each bulge. The scanning was repeated four times before changing the orientation of the defects in a descending manner. Computing the average across the flat surface profile of each protrusion yielded the measured mean height. The percentage difference between the mean measured height and the actual measurement was used to calculate the error (see Table 3). The findings indicated that the measuring equipment was able to accurately record surface variances within its sensing range with an average measurement error of less than 5%.

Table 3 Validation results for error percentage of each defect

	Mean height measured (mm)				
Scan #	Mean A	Mean B	Mean C	Mean D	Mean E
Scan #1	0.462	1.136	1.818	3.256	6.397
Scan #2	0.485	1.065	1.774	3.222	6.388
Scan #3	0.498	1.058	1.784	3.223	6.385
Scan #4	0.500	1.029	1.721	3.098	6.306
Actual	0.49	1.07	1.75	3.1	6.1
	Error %				
Scan #1	5.758	6.147	3.909	5.018	4.876
Scan #2	0.948	0.467	1.371	3.943	4.724
Scan #3	1.676	1.078	1.920	3.978	4.675
Scan #4	2.114	3.810	1.646	0.072	3.370
Avg	**3.23**	**3.28**	**2.21**	**3.25**	**4.41**

Ascending

	Mean height captured (mm)				
Scan #	Mean E	Mean D	Mean C	Mean B	Mean A
Scan #1	6.268	3.182	1.826	1.123	0.504
Scan #2	6.237	3.168	1.820	1.134	0.51
Scan #3	6.218	3.174	1.833	1.122	0.508
Scan #4	6.183	3.148	1.784	1.112	0.507
Actual	6.1	3.1	1.75	1.07	0.49
	Error %				
Scan #1	2.750	2.647	4.317	4.950	2.857
Scan #2	2.240	2.202	4.000	5.988	4.082
Scan #3	1.931	2.380	4.762	4.898	3.673
Scan #4	1.366	1.557	1.968	3.911	3.469
Avg	**2.07**	**2.20**	**3.76**	**4.94**	**3.52**

Descending

3.2 Sample with various roughness

The second experiment was conducted on three samples, each with a different level of surface roughness (see Fig. 7). A continuous non-zero magnitude height was recorded in the scan output because zero-reset is not performed prior to scanning. The objective of this experiment was to look for differences in the surface profile captured for surfaces with different roughness.

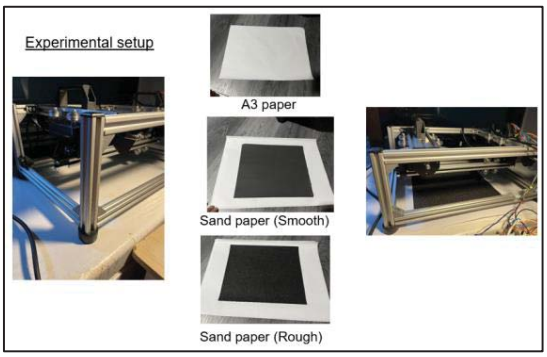

Fig. 7 Setup for various samples

From the results obtained below, the surface profile of the table surface had slight differences as compared to the smooth sandpaper, whilst more evident deviations were visible for the rough sandpaper. Based on the results shown in Fig. 8, the scanning device was able to record the various surface profiles for variances of about 0.4mm.

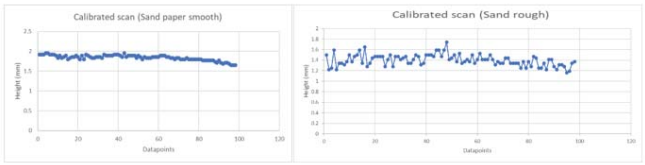

a) b)

Fig. 8 Surface profile captured for varying surface texture for (a) Smooth sandpaper and (b) Rough sandpaper

3.3 Samples with both bulges and depressions

The third experiment was conducted on surface containing both bulges and depressions. For testing, each scanning sequence only executed one scan line. By reconstructing the surface profile, the goal was to determine the capability of the device in distinguishing both bulges and protrusions with the same surface. This preliminary examination was entirely visual as it did not require for any surface parameter computation. Figs. 9 and 10 were the samples used in the preliminary analysis that included both simulated depressions and protrusions, as well as measurements of regular and irregular bulges.

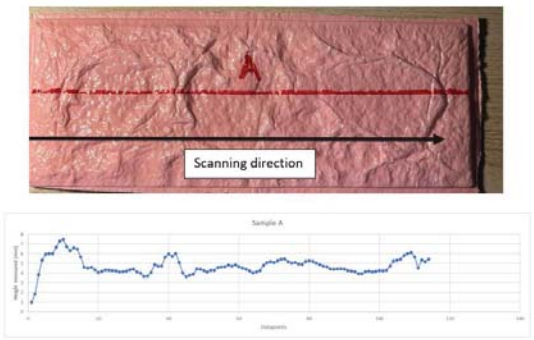

Fig. 9 Sample simulating concrete surface and reconstructed profile using the device

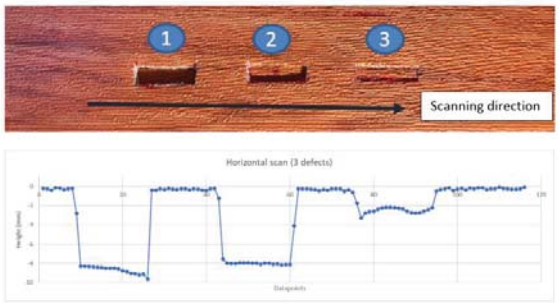

Fig. 10 Sample with man-made depressions and reconstructed profile using the device

For both types of surface defects (see Figs. 9 & 10), the results indicated that the device was capable in capturing the man-made defects. To further characterize the surface profile obtained, roughness parameter computation could be performed for average roughness and root-mean-square roughness.

4. Conclusion

This paper presented the design and development of a surface roughness device for rough and porous surface. The development of the measurement device involved several tests and experiments, from simple surface reconstruction to surface roughness computation and validation. While the preliminary tests were run using the standard horizontal scanning procedure, the results demonstrated that the developed device was able to capture and recreate the surface profile of the scanned sample for both depression and protrusion defects for the geometrical analysis. Hence, the proposed device was able to effectively reconstruct surface profiles and perform analysis of the surface roughness.

While the developed device was able to perform scanning and general evaluation of the surface characteristic, there were several areas for future work, and these include the following: (i) Enhancing the scanning acquisition rate to further increase the accuracy, (ii) Exploring different scanning path patterns to optimize the scanning time, and lastly (iii) Enhancing the design of the measurement device to make it lighter.

REFERENCES

1. Pedro M.D. Santos, Eduardo N.B.S. Júlio, “A state-of-the-art review on roughness quantification methods for concrete surfaces,” Construction and Building Materials, Volume 38, 2013, pages 912-923, ISSN 0950-0618
2. Hoła. Jerzy, Sadowski. Lukasz, Reiner. Jacek, Stankiewicz. Maciej, “Concrete surface roughness testing using nondestructive three-dimensional optical method.”, pages 101-106, 2012.